

The central Arctic Ocean as a source of dimethyl sulfide Seasonal variability in relation to biological activity

By CAROLINE LECK* AND CECILIA PERSSON, *Department of Meteorology,
Stockholm University, S-106 91, Stockholm, Sweden*

(Manuscript received 21 June 1994; in final form 31 August 1995)

ABSTRACT

Seawater dimethyl sulfide (DMS) and distribution of phytoplankton biomass were investigated in relation to sea ice conditions, hydrography and nutrients, onboard the Swedish icebreaker *Oden* as a part of the International Arctic Ocean Expedition, 1991. The expedition lasted from the beginning of August until the middle of October and covered sampling between 75 to 90°N in the open waters and along the ice edge zone in the Greenland Sea-Fram Strait area as well as in the pack ice of the western part of the Nansen and Amundsen basins and in the Makarov basin. Surface seawater DMS concentrations showed a clear seasonal progression related to biological activity, ranging from 0.04 to 12 nmol dm⁻³. The highest values were found in open waters along the ice edge in the beginning of August, while the lowest concentrations were measured beneath heavy pack ice in late September. On average DMS fell about 30% per week in the open waters south of and within the ice edge zone whereas a significant higher seasonal decline, about 45% per week, was observed in the pack ice during freeze-up. The importance of the phytoplankton bloom and zooplankton abundance both at the ice edge zone and in the pack ice during summer ice-melt to DMS concentrations in seawater has been demonstrated. We also demonstrated a potential for intense DMS production in the open waters in the wake of the receding ice. The extremely low surface concentrations of DMS during the freeze-up of the pack ice were probably primarily controlled by removal processes within the water column. The turnover time of DMS in the pack ice water column was calculated to be of the order of 13 days with the most effective sink seemingly of micro-biological origin. Although, our limited set of data indicated the likelihood of a relationship between DMS and degraded phytoplankton material (phaeopigments), seawater DMS showed no simple correlation with phytoplankton standing stock over the large areas and different seasons covered. The area weighed summer and winter fluxes of DMS from the Arctic Polar Ocean to the atmosphere were estimated to be 2.0 and 0.03 μmol m⁻² day⁻¹, respectively. On an annual basis, winter biogenic sulfur emissions are negligible compared to the summer emissions in the region. The total emissions of marine biogenic sulfur from the Northern Hemispheric high latitudes was estimated to be approximately 4 Gmol yr⁻¹.

1. Introduction

Over the last decade, increasing attention has been focused on oceanic emissions of dimethyl sulfide (DMS) to the atmosphere, as its significance in precipitation chemistry was realised, and a possible role in climate control invoked (Charlson and Rodhe, 1982; Charlson et al., 1987). This makes

it important to understand the processes controlling the cycling of reduced sulfur in surface seawater.

Phytoplankton is generally believed to be the major source of DMS in the oceans. DMS derives from enzymatic cleavage of β-dimethylsulfonio-propionate (DMSP), which was originally identified in phytoplankton (Challenger and Simpson, 1948) and in marine macro algae (Challenger et al., 1957). The similarity in structure and chemical behaviour between intra-cellular DMSP and

* Corresponding author.

glycine betaine suggest an osmoregulatory role (Vairavamurthy et al., 1985; Dickson and Kirst, 1986). Moreover, the findings by Kirst et al. (1991) in Antarctic macro algae suggest an additional role of DMSP as a cryoprotectant in polar waters.

The generally poor correlation between parallel measurements of DMS and chlorophyll *a*, phytoplankton primary production and biomass have been explained as a consequence of the species specificity of DMS production (Turner et al., 1988). The suggestion that DMS is most probably produced from extra-cellular DMSP and not from intra-cellular DMSP (Turner et al., 1988; Kiene, 1992) could be a further reason for the poor correlation between DMS and chlorophyll *a* concentrations. In addition, it appears that DMS is primarily released from algae upon cell lysis, bacterial attack or grazing (Dacey and Wakeham, 1986; Nguyen et al., 1988; Leck et al., 1990).

Once produced, DMS in the surface mixed layer will be exposed to removal processes. These include photochemical oxidation (Brimblecombe and Shooter, 1986) micro-biological degradation (Kanagawa and Kelly, 1986), ventilation to the atmosphere, advection and vertical mixing. The concentration of DMS in surface seawater appears to be primarily controlled by the biological cycling of DMS and DMSP with biological turnover times of about 1–2 days (Kiene and Bates, 1990; Leck et al., 1990).

Many DMS measurements have been made in transects covering coastal, shelf and open ocean areas. These measurements show that DMS is the major source of biogenic sulfur in seawater but that considerable temporal and spatial variability occurs (Andreae 1986; Bates et al., 1987; Turner et al., 1988; Cooper and Matrai, 1989; Leck et al., 1990; Leck and Rodhe, 1991). Recent global estimates of DMS flux from the oceans range from 250 to 1600 Gmol S yr⁻¹ (Andreae, 1986; Bates et al., 1987; Spiro et al., 1992). This accounts for at least 50% of natural emissions from ocean, plants and soils taken together (Bates et al., 1992). Altogether the natural sulfur flux is estimated to be of the same order of magnitude as the anthropogenic sulfur emissions, mainly from fossil fuel combustion, which are currently estimated at 1950–2500 Gmol S yr⁻¹ (Möller, 1984; Hameed and Dignon, 1988). The relatively large uncertainty in the reported estimates of the oceanic DMS flux is partly due to differences in the transfer

velocities used in the sea to air calculations, but mainly to the different assumption made when making seasonal and latitudinal extrapolations of the DMS seawater measurements. In particular, there is a paucity of data for seawater DMS concentrations in the winter months and at high latitudes.

High latitude oceans are characterised by their extremes in environmental conditions for marine life: extreme seasonal fluctuations in solar irradiance and day length, low seawater temperatures and the presence of a seasonal or permanent ice cover. These factors impose limits on productivity and growth rate, resulting in generally lower species diversity and higher abundance of species present. In regions with perennial or seasonal ice cover, phytoplankton growth is restricted to the short melting period in spring and summer. Moreover, the ice edge zone (IEZ), the region of seasonal melting, is known as an area of intense biological activity and enhanced standing stock (Smith and Nelson, 1985).

This study, which represents an addition to the Northern Hemispheric high latitudinal (75–90°N) data base on seawater DMS, chlorophyll *a*, and phaeopigments (degraded plant material), was undertaken in order to investigate the relationship between phytoplankton standing stock and the DMS concentrations over a seasonal progression. Further, their magnitude and distribution in relation to nutrient supply and water mass origin will be discussed. Based on the DMS data, sea-to-air fluxes of DMS for the open water, the IEZ and the pack ice of the central Arctic Ocean are calculated and an estimate is given of the potential DMS flux from the Arctic Polar Ocean divided into two seasons, summer and winter.

The measurements were undertaken as part of the Atmospheric programme during the International Arctic Ocean Expedition (IAOE-91), summer and fall of 1991, and were made together with atmospheric gas and condensed phase physical and chemical measurements with the focus on understanding the natural atmospheric sulfur cycle and its potential control on climate.

2. Experimental approach

The boundaries of the Arctic Polar Ocean are defined by the American continent, the Canadian

Arctic Archipelago, Greenland, Spitsbergen, the northern cape of Novaja Zemlja and the Eurasian continent along the Siberian coast (cf. Fig. 1.). The Arctic Polar Ocean consists of the central Arctic Ocean, the Canadian Arctic Archipelago, the Greenland Sea, and the Kara and Barents seas. The central Arctic Ocean basin (including the Laptev, East Siberian, Chukchi and Beaufort seas) is divided by the Lomonosov ridge into two major deep water basins, the Eurasian and Canadian, and of the marginal seas, which with their shelves compose as much as 1/3 of the total area of about 10^7 km^2 . The exchange of water with the rest of the world oceans is mainly through four restricted

passages, the Canadian Arctic Archipelago, the Fram Strait, the Barents Sea and the Bering strait.

During the 67 day cruise from 1 August to 6 October, about 15 days were spent in the open waters of the Greenland Sea and at the IEZ in the Fram Strait region, and the rest of the time in the pack ice of the western part of the Nansen and Amundsen basins, with a short visit to the Makarov basin. Measurements were performed aboard the Swedish icebreaker *Oden* during 13 separate 24-h sampling periods, and frequently in between since it was possible to combine sampling within the atmospheric programme with other programmes aboard, cf. Fig. 1.

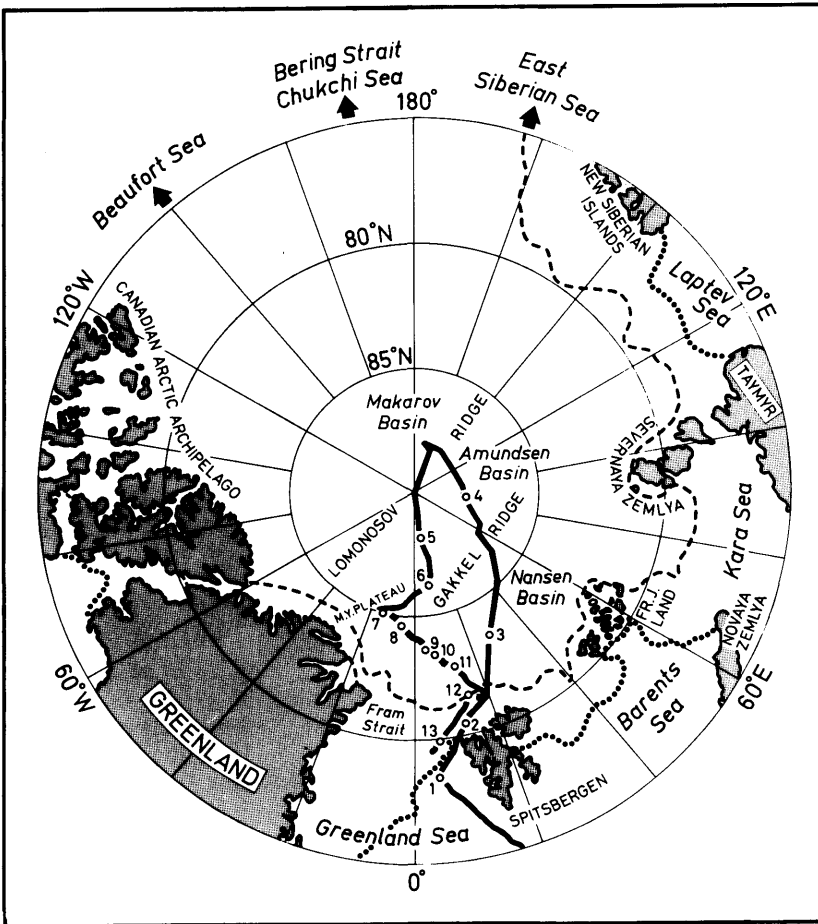


Fig. 1. Map of the study area, showing the cruise track during the International Arctic Ocean Expedition, 1991 (IAOE-91). Stations with 24 h continuous sampling are marked. Also illustrated is the geographical distribution of the most southerly (.....) and the most northerly (---) location of the ice edge zone during the expedition.

Samples of salinity, temperature, nutrients, chlorophyll *a*, and phaeopigments were in general collected from the ship side with a 12 rosette bottle 10 dm³ Niskin type, CTD instrument (Niel Brown), from a minimum of 8 depths from the surface down to 200 m, and during 25% of the stations processed from the same water sample as determined for seawater DMS. For better resolution, additional samples for chlorophyll *a*, and phaeopigments were taken with a Teflon coated water sampler (Ruttner) from depths between 0 and 50 m. Seawater bulk samples of DMS were also collected with the Ruttner sampler from a depth between 4 and 10 m, either from the ship side or for better horizontal resolution with a small motorboat (near the ice-breaker) or from a helicopter (leads within the pack ice up to 50 km from the ice-breaker).

Within 48 h of sampling, the analyses of salinity were performed with a Guildline AutoSal salinometer. The analytical accuracy was better than ± 0.002 psu (practical salinity units). Nutrient (nitrate, silicate and phosphate) analyses were made according to standard routines with a Technicon Autoanalyzer (Kattner and Becker, 1991). The precision of the technique was better than 0.05 μM for nitrate and silicate, and better than 0.01 μM for phosphate.

For determination of chlorophyll *a* and phaeopigment concentrations (indicating phytoplankton biomass and degraded plant material, respectively), usually 1 dm³ of seawater was filtered through a glass fiber filter (Whatman GF/C). After grinding and extracting (90% acetone, Sigma), the filtered samples were analysed on a Turner fluorometer.

Aliquots of DMS samples were loaded into a Pyrex glass sample chamber (200 cm³) via a depth filter using a peristaltic pump. Under the force of a nitrogen (N₂) stream the sample was then transferred into a Pyrex glass gas stripper. DMS and other reduced sulfur compounds were then purged from the sample using N₂ gas (600 cm³ min⁻¹) for 20 min and pre-concentrated in a U-shaped Pyrex glass cold trap (packed with glass beads) which had been placed in liquid argon. The samples were analysed using gas chromatography with flame photometric detection. A Chromosil 330 column was used to achieve near base-line separation of methyl mercaptan, carbon disulfide, DMS, and dimethyl disulfide (Leck and Bågander, 1988).

During IAOE-91 the main compound present was DMS (about 98% of total reduced sulfur), therefore we here on only will discuss the result of DMS. The detection limit for DMS was 0.006 nmol dm⁻³. The variability (given as one standard error of the mean) for samples collected from a helicopter and small motorboat were 30% and 10%, respectively.

Ancillary measurements included surface seawater mixed layer temperature, and hourly or half-hourly meteorological surface observations of wind speed and direction and wet and dry bulb temperature. Detailed information regarding prevailing ice conditions during the expedition is given by Liljeström (1992) and Carlström and Ulander (1993). Additional ice information was obtained from satellite images from both the NOAA-11 AVHRR (Advanced Very High Resolution Radiometer) and the GOES-7 (NESDIS/Synoptic Analysis Branch). Furthermore, we used ice maps prepared by the Norwegian Meteorological Institute.

3. Results and discussion

3.1. Factors influencing biological activity in the central Arctic Ocean

This paper is concerned only with biological activity and the result of DMS concentrations in the top 200 m layer of the ocean. Within in this layer, biological activity is influenced by such factors as depth of the surface mixed layer (SML) and stratification below it, ice conditions, available light and nutrient concentrations. Water temperatures vary only over a small range in the presence of ice. All these factors are in turn influenced by the general oceanic circulation. In order to discuss the observed changes in DMS concentrations in the water it is therefore necessary to consider first how they influence biological activity and then how they varied during the expedition.

3.1.1. The SML and the underlying halocline. The formation of a highly stable SML prevents the transport of phytoplankton to depths where there growth is light limiting (generally below 30–50 m according to Svedrup, 1953) and is therefore a factor important to biological activity. In polar seas its formation is dominated by melting and freezing with the consequent variations in relative density of the water. The relatively low density of the SML in summer is due partly to runoff of melt waters of

low salinity (1–4 psu) into the open leads and partly due to continental runoff of fresh water from Siberian and other rivers. As winter approaches salt is again frozen out as the open leads freeze, leading to a rise in density at the surface with consequent convection. Immediately below the SML is a cold upper and lower halocline with temperatures close to the freezing point to about 100 m, in which salinity increases rapidly from the low values of the SML to 34 to 34.5 psu at 100 m and about 34.5 to 53 psu at 200 m.

The general circulation of the SML in the central Arctic Ocean, as indicated by ice drift observation, is anticyclonal while the flow of the halocline and the Atlantic deep water is cyclonal. A more detailed overview of water masses and circulation in the Eurasian basin during the IAOE-91 can be found in Anderson et al. (1994).

3.1.2. Seasonal changes in ice conditions. The amount of light available for biological growth is of course very strongly seasonal in polar regions. This seasonality is enhanced by the corresponding changes in ice cover, the formation of melt pools and the removal of dry snow in summer which greatly increase the available radiation at a given depth in the sea (English, 1961). The changes in ice conditions encountered during the cruise are therefore likely to be very important to biological activity, influencing both available light and the depth of the SML. To simplify their description, four zones are distinguished: open water zone (OWZ), open ice edge zone (OIEZ), inner ice edge zone (IIEZ) and the closed pack ice zone (CPIZ). Melting is rapid at the IEZ in Fram Strait where the cold east Greenland current carrying a considerable amount of ice out of the central Arctic Ocean meets the opposing north west flow of the north Atlantic Current (West Spitsbergen current) and is further enhanced by up-welling and down-welling motions resulting from wind interactions (Johannessen et al., 1983). Fig. 1 illustrates the geographical distribution of the most southerly (early August and October) and most northerly (late August through early September) location of the IEZ during the IAOE-91 expedition.

When we entered the pack ice on 17 August (Julian Day 229; 81.5°N at 19.8°E) after a delay in Spitsbergen, the OIEZ was 70 to 80 km wide and had about 2/10 of floes classified as ice cakes, with thicknesses up to about 0.8 m. Ice cover in the about 90 km wide IIEZ as typically between 4/10

and 8/10 and consisted of larger floes than in the OIEZ with thicknesses of up to 1 m. The position of the ice edge retreated north by about 130 km during the period 17–27 August so that the quoted widths of OIEZ and IIEZ would have been influenced by this movement.

In the CPIZ (defined as the area with an ice cover of 8/10 or more), floes were up to several km in diameter, with thicknesses between 1.5 to 5 m (on average 2.5 m) and were interrupted by an irregular pattern of leads from a few metres up to 2000 m in width. Before 22 August (Julian Day 234; 650 km north of the OWZ), the area was dominated by first year ice, covered with wet snow. In addition, ponds of melt water were visible on the floes, estimated to cover from 20 to 40% of the floe surface. Between 22 to 27 August (beyond 650 to 1200 km from the OWZ) we encountered gradually tougher ice conditions in general showing a surface layer of multiple year pack ice, consisting of recrystallised low density ice and recently frozen melt ponds (from 10–20% to 5–10%; beyond 1000 km from the OWZ) underneath a thin and dry snow cover (0.06 m).

From 9 September (Julian Day 252; close to the North Pole), all pond surfaces were frozen, the leads began to freeze, and the area was covered with the snow of a new winter, that is in an early freeze-up phase. On rare occasions during the freeze-up period, open leads caused by ice drift, with a breadth of about 1000 m, were observed.

When moving out of the pack ice on 29 September (Julian Day 272; 82.7°N at 13°E) the ice cover changed rapidly. North of 100 km from the OWZ the ice cover was between 9/10 to 10/10. As a result of the late season, the ice cover in the 50 km wide IIEZ was less than 9/10, in general 7/10, with up to 70% multiple year ice. The <50 km broad OIEZ showed only small amounts (1/10–2/10) of single floes and floes in belt.

3.1.3. The importance of nutrient concentrations. While the increasing light and the formation of a stable SML in spring favour phytoplankton growth the melt also releases nutrients derived from winter storage. The peak in phytoplankton biomass is reached as nutrients in the SML approach exhaustion. After the initial bloom period it has been suggested by Niebauer and Alexander (1985) that biological productivity, in the wake of the ice receding towards higher latitudes, is maintained through the provision of

nutrients by upwelling and eddies. Moreover, the ice itself is a source of phytoplankton which can be released into the SML during melting and may act as an inoculum for blooms (Smith and Nelson, 1985).

Blooms in the IEZ of the southern Barents Sea may start as early as March–April due to light and contact with the relatively warm Atlantic water (Sakshaug and Slagstad, 1991). May and June blooms have been recorded in large parts of the Beaufort, Bering, Chukchi and Greenland seas. (Digby, 1953; Iverson et al., 1979). Episodic blooms have been observed until late August–September, caused by upwellings and eddies associated with the interaction between East Greenland and West Spitsbergen currents (Sakshaug and Slagstad, 1991).

3.2. Profiles of variables relevant to biological activity across the ice edge

Vertical profiles of salinity, temperature, nitrate, silicate, phosphate, chlorophyll *a* and phaeopigments along a transect across the ice edge can reveal the environmental constraints on biological activity and the effects of phytoplankton blooms. Two such transects are described, one moving into the pack ice and one leaving it.

3.2.1. The transect moving into the pack ice. This started in the OWZ at 81.5°N, 19.8°E on 17 August (Julian Day 229) and ended in the CPIZ at 86.6°N, 55.3°E on 27 August (Julian Day 239).

Salinity and temperature

Figs. 2a and 2e show the course of salinity and temperature along the transect. Low salinities of about 33 psu near the surface in the vicinity of the OIEZ and IIEZ indicated the combined effects of sea ice melting, river runoff and source waters. Stratification was intense as this low salinity water lay above a core of a warm, high salinity Atlantic water and the SML was only about 10 m in depth. Temperature showed little variation with depth, but were lower towards the north.

In the CPIZ 450–900 km from the OWZ the surface mixed layer was still shallow, only about 10–15 m. Salinity was higher (33.5 psu) than at the ice edge and increased more slowly with depth. Temperature remained almost constant at about -1.7°C to a depth of about 100 m, and then increased reaching 1°C at about 160 m. Anderson and Jones (1992) have discussed possible sources of water (river runoff, Atlantic water passing

through Kara and Barents seas, and sea ice melt) in this region.

At the northern end of the transect (900–1200 km from the OWZ) there was again a decrease in surface salinity to about 33.0 psu. Anderson et al. (1994) found that total carbonate values normalised to a salinity of 35 psu indicated that Siberian river runoff and transfer of this water by the Trans-Polar drift could account for the decrease. The surface mixed layer depth increased to 20–30 m while the temperature distribution remained much the same as in the previous section.

Nitrate, silicate and phosphate

The distributions of nitrate, silicate and phosphate along the transect were very similar (Figs. 2b, c, and d) with concentrations near the surface increasing from south to north. The lower nitrate and phosphate and higher silicate values found at the northern end of the transect in the CPIZ are consistent with the proposed influence of Siberian rivers.

The largest concentration gradients of these macro nutrients with depth were found in the upper halocline at depths between 50 and 100 m, while concentrations in the lower halocline between 160 and 200 m did not vary along the entire transect. These average concentrations of 11.7, 5.3 and $0.75 \mu\text{mol kg}^{-1}$ for nitrate, silicate and phosphate respectively can be used as an approximation of pre-bloom concentrations. They are consistent with reported data close to the Spitsbergen area (Anderson and Dyrssen, 1981) and differ little from the Redfield ratio (N:P, by atoms) of 16:1. Largest deviations from the Redfield ratio occurred in the SML of the OIEZ and IIEZ where inorganic nutrient concentrations dropped to levels near depletion. In the top 10 m average concentrations were 0.3, 1.3 and $0.15 \mu\text{mol kg}^{-1}$ for nitrate, silicate and phosphate, respectively.

*Chlorophyll *a* and phaeopigments*

Chlorophyll *a* and phaeopigment concentrations along the transect are shown in Figs. 2f, g. In general, inorganic nutrients along the transect were negatively correlated with autotrophic biomass indicating that uptake into biomass was the main factor in reducing inorganic nutrient levels in the euphotic (light penetration $>1\%$) zone. The spatial coherence between the layer of lowered salinity and the standing stock of phytoplankton as measured by chlorophyll *a* is evidence

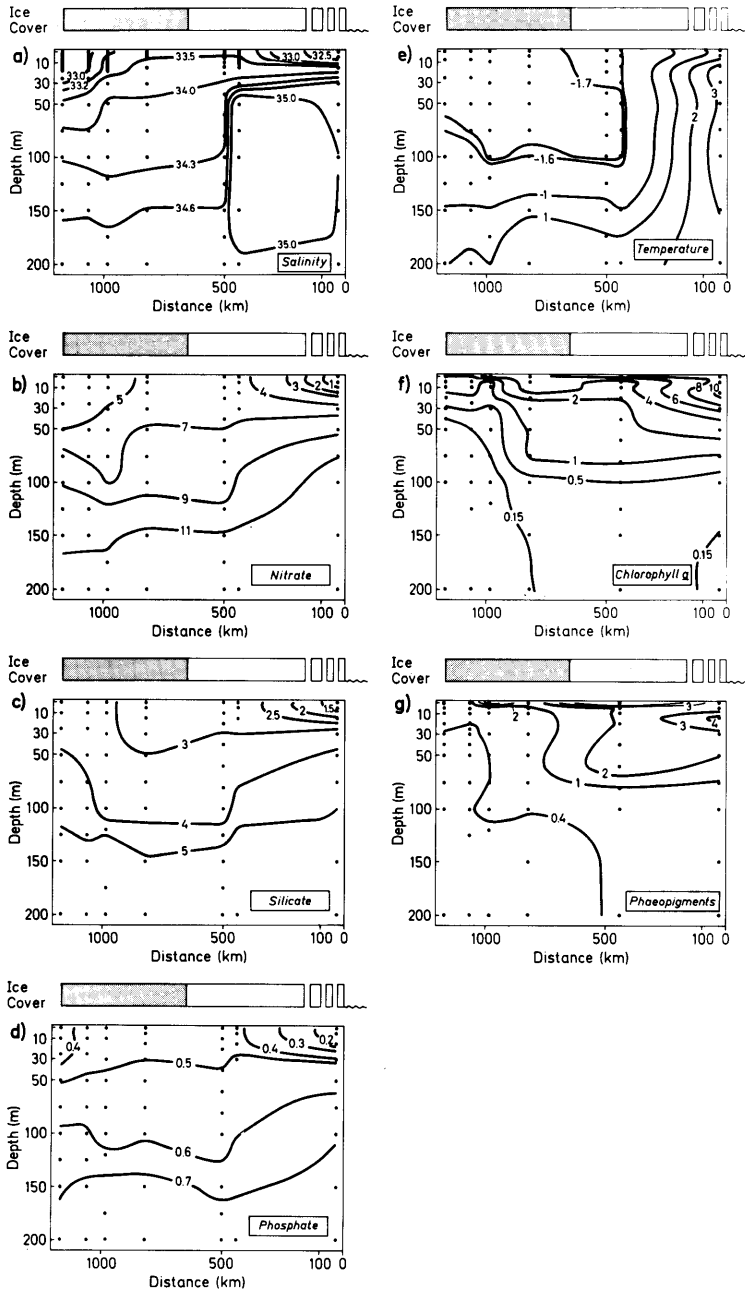


Fig. 2. Vertical sections of (a) salinity (psu), (b) nitrate ($\mu\text{mol kg}^{-1}$), (c) silicate ($\mu\text{mol kg}^{-1}$), (d) phosphate ($\mu\text{mol kg}^{-1}$), (e) potential temperature ($^{\circ}\text{C}$), (f) chlorophyll a ($\mu\text{g dm}^{-3}$), (g) phaeopigments ($\mu\text{g dm}^{-3}$) along the transect moving into the pack ice. The ice cover is presented as bars with mean ice concentrations as defined in Subsection 3.1.2. The open bars represents the area affected by ice-melt. Dots indicate sampling depth.

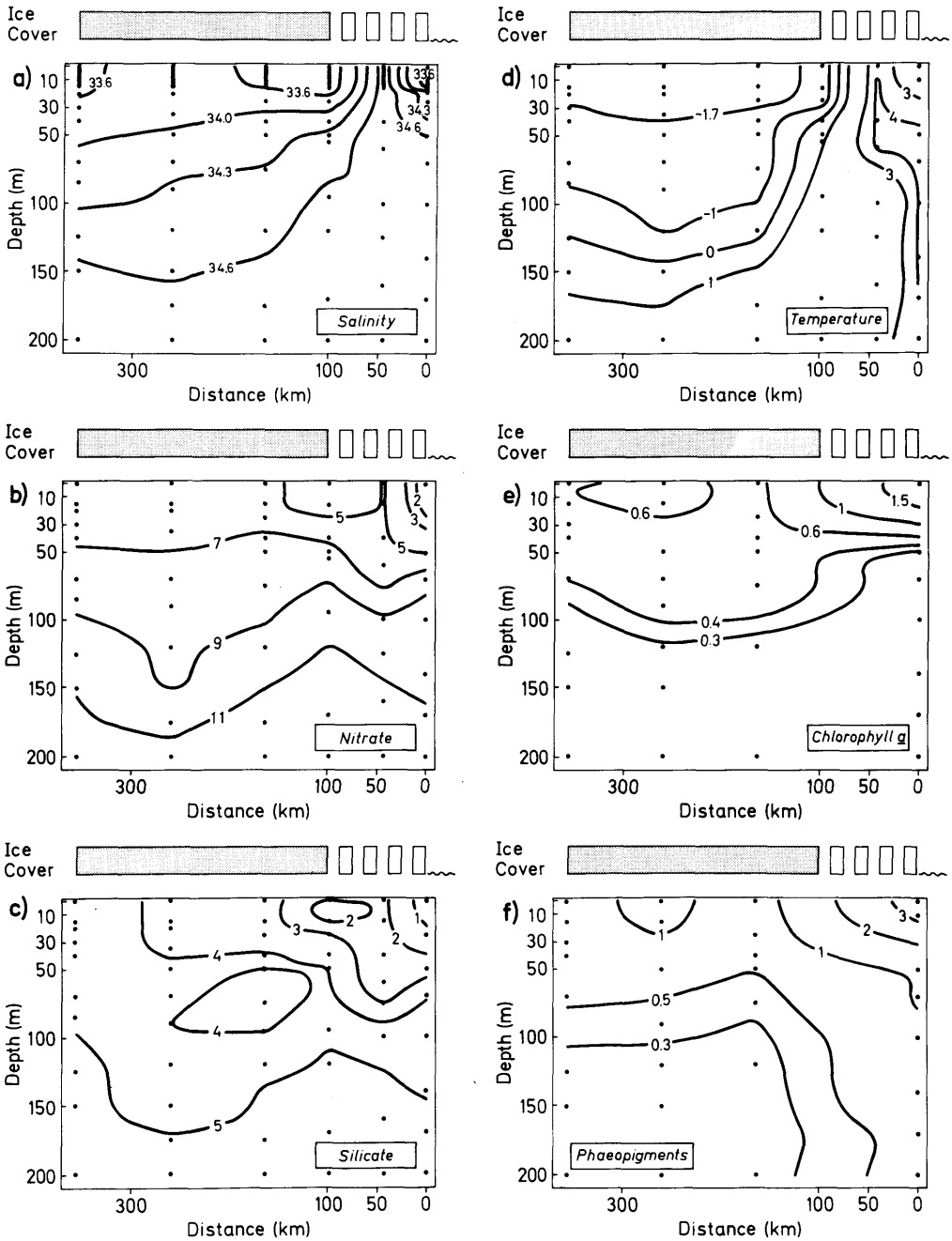


Fig. 3. Vertical sections of (a) salinity (psu), (b) nitrate ($\mu\text{mol kg}^{-1}$), (c) silicate ($\mu\text{mol kg}^{-1}$), (d) potential temperature ($^{\circ}\text{C}$), (e) chlorophyll *a* ($\mu\text{g dm}^{-3}$), (f) phaeopigments ($\mu\text{g dm}^{-3}$), along the transect moving out of the pack ice. The ice cover is presented as bars with mean ice concentrations as defined in Subsection 3.1.2. The open bars represents the area affected by ice-melt. Dots indicate sampling depth.

that phytoplankton and vertical stratification are causally related. Subsurface maxima in both chlorophyll *a* and phaeopigments were observed at most stations and the maxima corresponded to regions of rapid salinity change.

Strong indications of a bloom at its peak in the OIEZ included the high subsurface levels of $10.2 \mu\text{g dm}^{-3}$ of chlorophyll *a*, nutrient concentrations near depletion and the normalised total carbonate values (Anderson et al., 1994) as expected from primary production.

Phytoplankton growth beyond 1000 km from the OWZ was apparently inhibited because relatively low SML concentrations of $1\text{--}2 \mu\text{g dm}^{-3}$ of chlorophyll *a* accompanied high nutrient levels. There have been several studies of the availability of photosynthetically active light in the Arctic that suggest lack of light to have been an inhibiting factor. Maykut and Grenfell (1975) in a Beaufort Sea study suggested that structural changes due to melting and refreezing would reduce photosynthetically active light to less than 1% in the interior of perennial and multiple year ice. In the most northerly 200 km of our transect ice conditions were such that attenuation should have been at least as great as the maximum found in these studies. Slow growth of shade-adapted phytoplankton and negligible consumption of nutrients are likely to have resulted. The increased light available to the SML further south of 650 km along the transect (where the area was dominated by first year ice covered with wet snow interrupted by open leads and where meltponds were more numerous) was probably a major cause of the increased biomass observed.

The most obvious difference between chlorophyll *a* and phaeopigment distributions was the greater depth of the subsurface maximum in the latter. This was to be expected since phaeopigments are degradation products of chlorophyll *a* and therefore normally occurs below the chlorophyll *a* maximum. Summarising, the transect showed that a bloom of phytoplankton in the OIEZ and IIEZ was in progress and had severely depleted the nutrients, while further north (>1000 km from the OWZ) the decreasing availability of photosynthetically active light and the greater depth of the SML had inhibited phytoplankton growth.

3.2.2. The transect moving out of the pack ice. The outward traverse started in the pack ice on

29 September (Julian Day 272) at latitude 82.7°N , 13°E (station #11 on Fig. 1) and ended near open water at 81°N , 20°E on 5 October (Julian Day 278).

Salinity and temperature

The influence of water from different sources and ice-melt was again evident (Figs. 3a, d). These included the low salinity and the warm surface waters of the central Arctic Ocean and the West Spitsbergen current, while high silicate concentrations (Fig. 3c) at the northerly end of the transect suggested that Siberian rivers had again influenced salinity of that section. The somewhat higher (33.8 psu) salinity between the surface and 50 m of the region 200–300 km from the OWZ suggested some mixing of Atlantic and surface waters (Anderson and Jones, 1992). Stratification in the IIEZ may have been disturbed by upwelling that injected warm and highly saline Atlantic water. Temperature distributions and profiles also reflected these different water sources and resembled those of the inward traverse.

Nitrate and silicate

Only nitrate and silicate were available (Figs. 3b, c) and had similar distributions to those on the inward transect with low concentrations near the ice edge. Below 50 m, nitrate concentrations were again typical of pre-bloom winter conditions. This was also true of silicate although there was some enhancement in the upper 100 m.

*Chlorophyll *a* and phaeopigments*

Concentrations of both chlorophyll *a* and phaeopigments were low (Figs. 3e, f) in the CPIZ and the absence of a maximum below the surface indicated that the productive season beneath the heavy pack ice had ended. Concentrations ranged from 0.3–0.6 and 0.3–1 $\mu\text{g dm}^{-3}$ respectively in the upper 80 m averaging $0.5 \mu\text{g dm}^{-3}$ for both. Maximum concentrations in the water column of 0.3–1.5 and 0.5–3 $\mu\text{g dm}^{-3}$ respectively occurred in the OIEZ and were consistently associated with regions of rapid salinity change. Distributions of chlorophyll *a* was again reversible related to nutrient concentrations. Interesting to note is that the concentrations of phaeopigments exceeded those of chlorophyll *a*, thus indicating relatively high abundance of degraded plant material in the OIEZ. Lowest nutrient levels (about $1 \mu\text{mol kg}^{-1}$) occurred in the upper 15 m suggesting that some uptake by biomass had taken place there, in agreement with Heimdal's (1983) September findings in

the Fram Strait region. Chlorophyll *a* concentrations in the OIEZ were a factor of 5 lower than on the inward transect in August but the levels of phaeopigments remained much the same, suggesting that a loss of biomass probably followed after the peak phase of a bloom had occurred prior to the October sampling.

3.2.3. Measurements between the transects. Chlorophyll *a* concentrations were low (cf. Fig. 4a) between these two transects (Julian Day 240 to 271: stations #4, 5, 6, 7, 8, 9 and 10 in Fig. 1), values ranging between 0.6 and $1.8 \mu\text{g dm}^{-3}$ in the upper 30 m while it was more or less well-mixed at depths below 75 m. English (1961) has established from carbon-14 measurements that the photosynthetic potential of phytoplankton varies in a similar way to the amount of chlorophyll *a*. The phaeopigment concentrations (cf. Fig. 4b) however showed a higher degree of fluctuation ranging from 0.35 to nearly $2 \mu\text{g dm}^{-3}$. Highest concentrations were associated with the low salinity waters of the Makarov basin and the north-west part of the Amundsen basin towards the M. Y. Plateau. Consistently low concentrations were found in waters adjacent to the Gakkel ridge.

3.3. Surface seawater DMS of the central Arctic Ocean

The existence of a seasonal cycle in sea surface DMS has been reported in the literature (Turner et al., 1988; Leck et al., 1990). This cycle is pronounced in temperate latitudes with peak values occurring during the summer period. Average summer time DMS concentrations in the Baltic Sea and the North Sea ranged from 3 to 8 nmol dm^{-3} (Leck and Rodhe, 1991). During the expedition north of 80°N , we measured concentrations of between 0.04 and 12 nmol dm^{-3} sulfur, with peak values occurring in open waters along the ice edge in the beginning of August, cf. Fig. 4c. In the period following Julian Day 247, close to the North Pole, the DMS levels fell below 0.1 nmol dm^{-3} , i.e. concentrations typical for the winter season in the Baltic Sea (Leck et al., 1990). The lowest concentrations were measured beneath heavy pack ice in late September.

3.3.1. Observations in early August. The first set of DMS samples was obtained on 4 August (Julian Day 216; station #1 on Fig. 1) in the open water area west of Spitsbergen at a distance of

about 100 km from the IEZ. The surface layer was occupied by warm waters, on average 6°C and thus heavily influenced by the northward flow of the West Spitsbergen current. As shown in Fig. 4c, the concentrations of DMS on average measured $8.8 \pm 1.3 (1\sigma) \text{ nmol dm}^{-3}$. Similarly high DMS concentrations have been reported off the east coast off Greenland by Stabues and Georgii, (1993) and in the Bering Sea by Barnard et al. (1984). Water column content of chlorophyll *a* and phaeopigments for station #1 is shown in Fig. 5. Unfortunately no measurements of water column salinity, temperature, nitrate, silicate, or phosphate were made at this station, but it is reasonable to assume that an extensive vertical stability would be expected even without the presence of melting ice, as the pycnocline is a year round feature of this region. Upper surface water concentrations of both chlorophyll *a* and phaeopigments were low and comparable with levels found in September beneath the heavy pack ice and markedly lower than the maximum values found in the OIEZ when moving normal to the ice along the in-transect. A sharp increase in their concentrations was recorded between 45 m and 80 m. The column profile subsurface maxima at 80 m measured $3 \mu\text{g chlorophyll } a \text{ dm}^{-3}$ and $1.5 \mu\text{g phaeopigments dm}^{-3}$. Thereafter concentrations decreased with depth and reached $0.2 \mu\text{g dm}^{-3}$ and $0.5 \mu\text{g dm}^{-3}$ for chlorophyll *a* and phaeopigments respectively at 200 m.

Possible reasons for the low surface concentrations of chlorophyll *a* and phaeopigments seen in Fig. 5 include sedimentation, and zooplankton grazing and suggest a post-bloom situation. It can not be excluded that also lateral transport could in part explain the low surface phytoplankton values, and the subsurface maximum at station #1.

Nguyen et al. (1988), Keller et al. (1989) and Leck et al. (1990) showed from culture experiments and natural samples that healthy growing phytoplankton release little DMS and DMSP, while high levels of extra-cellular DMSP and DMS were associated with cell disruption by ageing and bacterial attack or grazing of senescent cells. While we have no information about the physiological state of the phytoplankton standing stocks during the IAOE-91 it is a reasonable assumption that the high surface concentrations of DMS during station #1 were associated with the senescent phase of a bloom since it is consistent

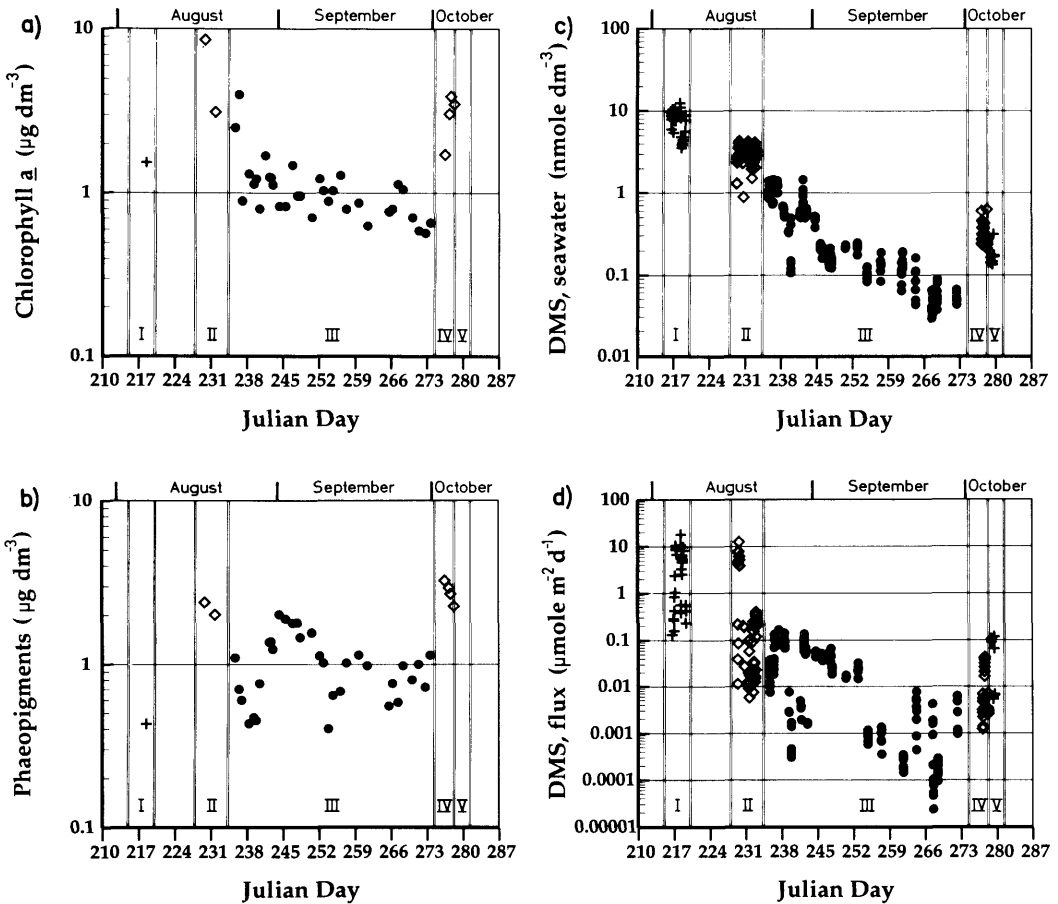


Fig. 4. Temporal distribution of surface mixed layer: (a) chlorophyll *a* ($\mu\text{g dm}^{-3}$), (b) phaeopigments ($\mu\text{g dm}^{-3}$), (c) DMS concentrations (nmol dm^{-3}) and (d) DMS flux ($\mu\text{mol m}^{-2} \text{d}^{-1}$) during August to October along IAOE-91. The periods in Roman numerals are defined as followed.

- I: Observations in early August in the OWZ.
- II: Observations in the OIEZ, IIEZ and CPIZ during summer ice-melt along the transect moving into the pack ice (cf. Fig. 2).
- III: Observations in the CPIZ, where IIIa represents the period between summer ice-melt and early freeze-up (Julian Days 235–250) and IIIb represents the period of early freeze-up (Julian Days 252–272).
- IV: Observations in the OIEZ and IIEZ along the transect moving out of the pack ice (cf. Fig. 3).
- V: Observations in early October in the OWZ.

with the profiles of chlorophyll *a* and phaeopigments.

3.3.2. *The transect moving into the pack ice.* The importance of the IEZ to DMS concentrations in seawater in the Antarctica has been shown by Gibson et al. (1990) and Fogelquist (1991). To assess the importance of the phytoplankton bloom of the IEZ discussed in Subsection 3.2.1., we now

present the DMS measurements made during that transect.

The concentrations of seawater DMS in the OWZ, in the middle of August, off the west coast of Spitsbergen increased as we approached the IEZ, cf. Fig. 6a. The samples collected at the ice edge showed similar levels to those measured two weeks earlier at station #2 (Fig. 1, 6 August,

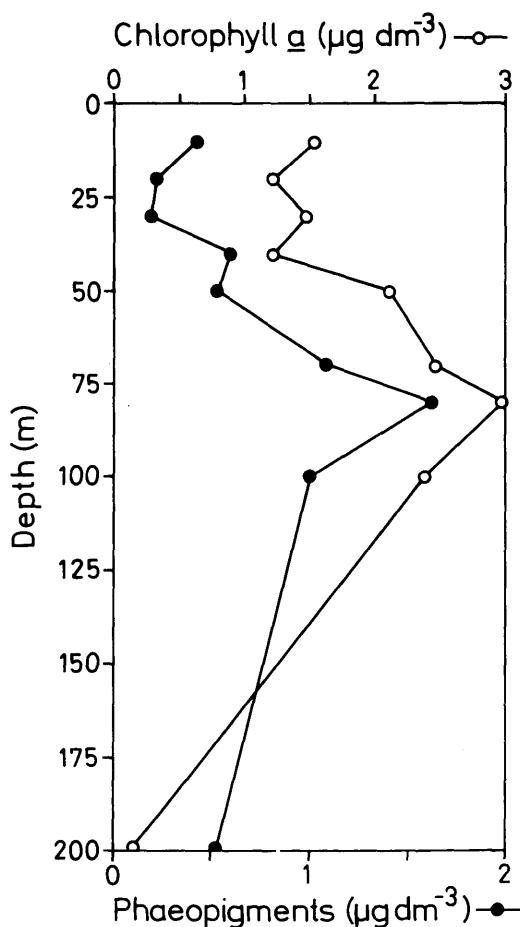


Fig. 5. Vertical distributions with depth of chlorophyll a and phaeopigments at station #1 on Fig. 1.

Julian day 218). Station #2 closely followed the first station in time but was closer to the IEZ. The SML was about 4°C cooler than at station #1 due to the influence of the southward flowing central Arctic Ocean water overrunning the warm West Spitsbergen current. Seawater concentrations of DMS were reduced to approximately half (4.3 ± 0.5 (1σ) nmol dm⁻³) of those of station #1 (cf. Fig. 4c).

Except for a few samples collected just at the edge of the CPIZ were we briefly encountered an area of multiple year ice and fewer melt ponds, concentrations of SML DMS remained at levels similar to those observed in the IEZ, as far as

500 km into the CPIZ, on average 3.0 ± 0.6 (1σ) nmol dm⁻³. As brought about by freezing of melt water ponds and leads and the dry snow cover, the decrease in pack ice submarine radiation was likely quite abrupt in late August. This not only led to a low and stable SML phytoplankton standing stock together with high levels of nutrients, but was also consistent with a factor of 6 lower levels of DMS measured beyond 1000 km from the OWZ.

Another potential factor that could control the abundance of phytoplankton standing stock and consequently DMS production is grazing by zooplankton. Both observations from field experiments (Leck et al., 1990) and culture studies (Dacey and Wakeham, 1986) have suggested zooplankton grazing on phytoplankton to be the major route by which DMSP enters the seawater for further conversion to DMS. As the abundance and biomass distribution of zooplankton was beyond the scope of this study we in the text below refer to results from bongo net hauls sampled along with the CTD casts during the expedition, reported by Hanssen (1993). Copepods were found to be the most important taxonomic group, with on average 84% of all individuals. Above average grazing rates were indicated on stations sampled along the transect within a distance of 650 km from the OWZ. This together with the relatively high abundance of phytoplankton biomass observed, is consistent with measured DMS concentrations in the CPIZ during ice-melt close to levels found in the open water in August.

3.3.3. *The transect moving out of the pack ice.* The distribution of SML DMS along the outward traverse in the beginning of October, showed maximum concentrations (0.34 ± 0.11 (1σ) nmol dm⁻³) in the IIEZ and OIEZ, cf. Fig. 6b. Levels of DMS were about 10 times lower than in the samples collected along the inward traverse in the middle of August. Hanssen (1993) found relatively high numbers of young *Calanus finmarchicus* indicative of herbivorous feeding in the OIEZ. Not much grazing activity was to be expected from the zooplankton composition in the CPIZ. Together with a low phytoplankton standing stock (discussed in Subsection 3.2.2), consistently very low (0.05 ± 0.007 (1σ) nmol dm⁻³; about 6 times lower than in the IEZ) DMS concentrations were measured beneath the heavy pack ice in late September.

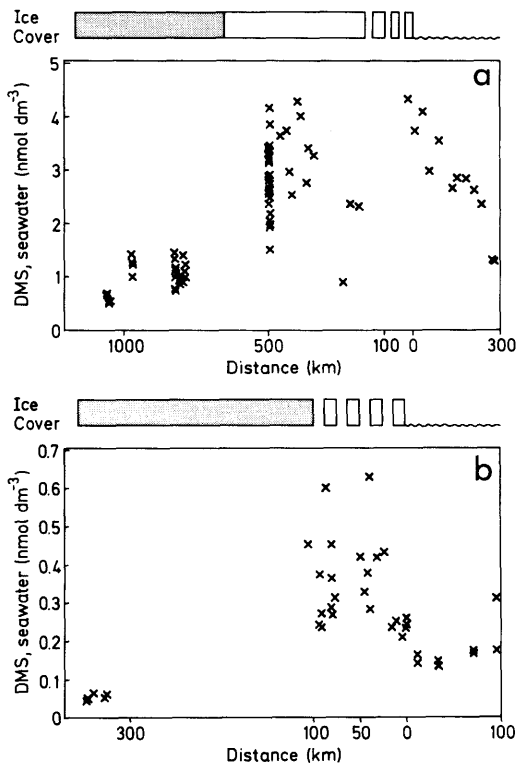


Fig. 6. Spatial distribution of surface seawater DMS: (a) along the transect moving into the pack ice and (b) along the transect moving out of the pack ice. The ice cover is presented as bars with mean ice concentrations as defined in Subsection 3.1.2. The open bars represents the area affected by ice-melt.

The last set of DMS samples was obtained in the OWZ on 6 October (Julian Day 279; station # 13 on Fig. 1.) As at station # 1 the water sampled was influenced by the northward flow of the West Spitsbergen current as indicated by water temperatures between 3 to 5°C. Surface mixed layer DMS concentrations were reduced to about half (0.17 ± 0.05 (1σ) nmol dm^{-3}) of those measured at the IEZ. Thus on average only 2% of the levels found at station # 1 in early August were observed 2 months later in the Fram Strait-Greenland Sea region.

3.3.4. Measurements between the transects. Concentrations of SML DMS were low between the two transects, decreasing with season from 1.5 to 0.04 nmol dm^{-3} (cf. Fig. 4c). In spite of

the large horizontal gradients in SML salinity encountered, reflecting the influence of different source waters, we found no clear connection between DMS and the biological and physiological parameters measured, except in the samples collected adjacent to the Gakkel ridge where low levels of phaeopigments coincided with low DMS concentrations. The abundance of SML DMS seemed to be more related to the gradual seasonal reduction in biological activity imposed by the rapid freeze-up of the pack ice.

Samples collected in leads covered with a thin layer of new ice showed about 50% higher DMS levels compared to samples collected beneath the heavy pack ice. This again shows the likely effect of the perennial ice in retarding phytoplankton growth and thus also decreasing zooplankton abundance and DMS production. It is thus reasonable to assume that the turnover of DMS within the CPIZ is not primarily controlled by new production but rather by removal processes. Following the assumption of zero production the turnover time (Bolin and Rodhe, 1973) for DMS in the SML was calculated to be of the order of 13 days. The turnover time caused by ventilation to the atmosphere was estimated to be of the order of 150 days (from Table 1; period III).

Thus the most effective removal process seems to be of micro-biological origin with an estimated turnover time of about 14 days and therefore about 10 times more important than atmospheric ventilation in controlling DMS concentration in the ocean and hence its emission to the atmosphere. The 14-day turnover time of this study is considerably longer than the 1 to 2 days that have been observed elsewhere in the world oceans (Kiene and Bates, 1990; Leck et al., 1990).

If DMS was primarily controlled by biological cycling within the water column, the CPIZ should exhibit a stronger seasonal decline of DMS than the biologically active ice edge and open water zones. On average, DMS concentrations fell about 45% per week ($r^2 = 0.78$, $P < 0.001$) during the duration of the transect. In comparison, a significantly lower seasonal exponential decline, about 30% per week ($r^2 = 0.93$, $P < 0.001$), was found in the open waters south of and within the ice edge zone.

3.3.5. Correlation between surface water DMS and phytoplankton biomass. No significant overall correlation between DMS concentration and

Table 1. Mean and one standard deviation () for input parameters used to calculate DMS fluxes for IAOE-91

	Time Julian day	No. of samples	DMS seawater (nmol dm ⁻³)	1-(Ca H ⁻¹ Cw ⁻¹) (%)	Water temperature (°C)	Wind speed (m s ⁻¹)	K _w (cm h ⁻¹)	Fraction open water (%)	Flux* (μmol m ⁻² day ⁻¹)
period I	216-219 Aug. 4-Aug. 7	37 [29]	7.9 (2.4)	97 (3)	4.8 (2.4)	3.9 (3.0)	2.3 (2.9)	100	3.3 (4.4)
period II	229-233 Aug. 17-Aug. 21	44 [43]	2.9 (0.73)	97 (3)	-1.2 (1.1)	4.1 (1.7)	1.5 (1.7)	17 (14)	0.31 (0.95)
period III	235-272 Aug. 23-Sept. 29	178 [164]	0.39 (0.38)	82 (16)	-1.6 (0.1)	5.3 (3.1)	3.1 (3.2)	11 (7)	0.027 (0.035)
period IIIa	235-250 Aug. 23-Sept. 7	107 [101]	0.58 (0.38)	89 (9)	-1.6 (0.1)	6.1 (3.1)	4.0 (3.4)	12 (6)	0.043 (0.037)
period IIIb	252-272 Sept. 9-Sept. 29	71 [63]	0.10 (0.057)	71 (18)	-1.7 (0.1)	4.1 (2.5)	1.7 (2.4)	10 (8)	0.003 (0.007)
period IV	276-278 Oct. 3-Oct. 5	24 [24]	0.34 (0.11)	99 (2)	-1.7 (0.1)	4.3 (1.4)	1.4 (1.6)	15 (11)	0.012 (0.014)
period V	278-279 Oct. 5-Oct. 6	10 [10]	0.17 (0.053)	97 (1)	4.4 (0.8)	3.6 (1.4)	1.2 (1.2)	100 (100)	0.050 (0.049)

* The fluxes are calculated for individual DMS water samples. In brackets [] are the number of samples with $U > 0.5 \text{ m s}^{-1}$. For the definition of period I-V, cf. legend, Fig. 4.

chlorophyll *a* or phaeopigment concentration was observed when the whole data set for the expedition was analysed. When data were grouped into samples collected from the two transects normal to the IEZ, still no correlation of DMS with chlorophyll *a* was found. However, the Spearman rank correlation coefficient *r* for the relation of DMS and phaeopigment concentration for the in-transect was 0.93 (*n* = 7), while that of the out-transect was 0.92 (*n* = 8). Both the correlation coefficients were significant at *P* < 0.001. One conspicuous result was that although the phaeopigment concentration and zooplankton standing stocks were nearly at the same level during both transects, levels of DMS were found about one order of magnitude higher in the middle of August than in the beginning of October. Nevertheless, these two as yet small sets of data indicate a relationship between DMS and degraded phytoplankton material. However, over larger areas or in different seasons, large variations in the production, consumption and conversion pathways of seawater DMSP and consequently DMS will occur. Thus, the processes controlling the cycling of sulfur in surface seawater must be looked upon as the result of complex physiological as well as ecological interactions and can not be expected to be simplistically associated with phytoplankton standing stock.

3.4. Dimethyl sulfide air-sea flux estimates

3.4.1. Assumptions underlying the flux estimates of DMS in partially ice-covered regions. Calculation of the sea to air flux of DMS in the remote Arctic environment poses some special difficulties that need to be discussed. For a moderately soluble gas such as DMS the interfacial gas air-sea flux is controlled by the resistance in the liquid phase. Liss and Slater (1974) used the following equation:

$$F = K_w(C_w - C_a H^{-1}), \quad (1)$$

where K_w is the transfer velocity, C_a and C_w the DMS concentration in air and in water below the interface and H the dimensionless Henry's law constant, expressed as the ratio of the concentration of gas in air to that in water at equilibrium. $C_a H^{-1}$ is therefore the concentration in water in equilibrium with the ambient air. For DMS over the open ocean, $C_a H^{-1}$ is at least two orders of magnitude less than C_w (Bingemer, 1984) so that

only C_w needs to be considered. However, in the remote ice covered central Arctic basin concentrations in water were low compared to atmospheric DMS (Leck and Persson, 1996) so that both terms must be included. We have used the Dacey et al. (1984) determined Henry's law constants for DMS and near-simultaneous measurements of DMS in air and water. Water samples collected in the melt ponds and within the ice showed negligible levels of DMS. We have thus assumed the ice itself to be no source of DMS to the atmosphere.

The most difficult problems in estimating sea to air flux from the partly ice covered central Arctic Ocean concern the transfer velocity, K_w . In the present study we used the relationship proposed by Liss and Merlivat (1986) to derive the K_w for DMS. The dependence of K_w on wind speed at 10 m has been parameterised from lake and wind-tunnel experiments for CO_2 at 20°C. The relationship is described in a combination of three linear segments having breaking points at 3.6 and 13 m s^{-1} , and distinguishes three types of roughness regimes: smooth surface, rough surface (onset of capillary waves) and breaking of gravity waves. In using the Liss-Merlivat relationship between K_w and wind speed for flux calculations from the open leads within the pack ice area, assumptions concerning the (a) the stratification of the MBL, (b) the effective wind fetch, (c) observed wind speeds (U) reduced to 10-m height, (d) surfactants and (e) the DMS diffusivity have to be made.

(a) Neutral stratification of the MBL was assumed as Nilsson (1996) has shown that a near neutral mixed layer was usually found near the surface. However stable stratification at the observing height of about 30 m was observed in air that had travelled less than ~400 km from the open water into the pack ice regions and Deardorff (1968) has shown that a suppression of air-sea exchange can occur with stable stratification. However, the surface roughness and wind speeds should counteract this suppression close to the surface.

(b) Work in lakes and wind wave tanks have shown that limited wind fetch gives reduced gas transfer (Wanninkhof, 1992). During IAOE-91 the open water within the pack ice consisted of an irregular pattern of leads, usually much longer than their width, having varying orientations to the wind. In the absence of statistical data on effective lead fetches the only possible approach is to

assume that fetch was unlimited on the open water. This is probably reasonable in that the largest expanses of open water (up to 2000 m across) accounted for a high proportion of the total open water. During the expedition the proportion of wind speeds above 13 m s^{-1} was less than 2%. Decreased flux in the gravity wave regime would therefore have been relatively unimportant. The observation of capillary waves at wind speeds of 3 m s^{-1} in a 30 m wide lead further reasons for a gas exchange unlimited by fetch within in the pack ice area.

(c) The Liss-Merlivat relationship between wind speed and K_w used winds measured at a height of 10 m over open water. During IAOE-91, the local wind speed were measured at a height of about 30 m over an ice surface of variable roughness. We have therefore normalised the winds to 10 m for two extremes, using a neutral drag coefficient (C_{dn}) for ocean of $1.5 \cdot 10^{-3}$ (Liss and Merlivat, 1986) and for extremely rough ice of $8.0 \cdot 10^{-3}$ (Guest and Davidson, 1991). The range in K_w was about 30%, being highest for the open ocean C_{dn} . We shall use the oceanic C_{dn} but include the effect of extremely rough ice as a probable error in the flux estimate.

(d) The effect of greasy ice (a soupy mass of unconsolidated ice crystals) in damping capillary waves are likely to reduce K_w (Guest and Davidson, 1991). To our knowledge, there have been no quantitative studies on the impact of greasy ice on K_w , but according to Goldman et al. (1988), transfer velocities can be reduced by as much as 80% by the presence of surfactance. As we have no information on special properties of the surface film of the ocean in partially ice-covered waters with its presence of greasy ice, its possible preventive effect on capillary waves and reduced air-sea exchange have been ignored in the K_w calculations. To estimate probable errors included in the ignored effect on gas transfer by the presence of greasy ice, we have assumed that greasy ice formed when air temperature dropped below -1.8°C . We have further assumed that there was no transfer of DMS to the air when greasy ice was present.

(e) As the Liss-Merlivat relationship between wind speed and K_w is valid for CO_2 at 20°C (Schmidt number, $Sc = 600$) it has to be corrected in accordance with the Sc for the gas under consideration. The Sc of that gas is the ratio of

kinematic viscosity to molecular diffusivity and n is the power law dependence such that $K_w = f(Sc^{-n})$. The relationship between K_w and Sc is also wind speed dependent such that $n = 2/3$ for $U < 3.6 \text{ m s}^{-1}$ and $n = 1/2$ for $U > 3.6 \text{ m s}^{-1}$. The Sc for DMS has been calculated for different temperatures according to the Saltzman et al. (1993) estimate of DMS diffusivity. Below these temperatures the diffusivities of DMS have been extrapolated.

3.4.2. Results. DMS fluxes have been calculated for individual samples using observed wind speed and sea surface temperatures. The calculated DMS fluxes were corrected for the known ice cover by multiplying eq. (1) with the fraction of open water present. The results are shown in Fig. 4d as a function of season. While there is an obvious seasonal change, detailed interpretation is difficult because of the dependence of flux on wind speed and the assumptions of Subsection 3.4.1. Because the individual fluxes are calculated from areas with different potential for biological activity and thus DMS production, in different ice conditions yielding fluxes with differing uncertainties, the fluxes are averaged over a number of defined periods (cf. legend as in Fig. 4) in Tables 1 and 2.

The flux of DMS to the atmosphere in early August (period I) showed an average of $3.3 \pm 4.4 \mu\text{mol m}^{-2} \text{ d}^{-1}$, while in early October (period V) the corresponding mean was almost 2 orders of magnitude lower ($0.050 \pm 0.049 \mu\text{mol m}^{-2} \text{ d}^{-1}$). The 10-fold decrease of the flux in period II as compared to period I was due to the imposed ice cover as we left the OWZ. The factor of 10 difference between period IIIa and IIIb would likely be attributed to the combined effect of lowered DMS concentrations, a close to 50% reduction in average wind speed and low DMS water concentrations compared to ambient atmospheric DMS levels.

When the errors relating to the assumptions ((c) and (d)) above were applied to the flux calculations, the reduced effect on gas transfer was found most pronounced in the CPIZ. For period III we found the extreme differences to cause a 60% reduction of the DMS flux. A similar number of 30% were estimated for both period II and IV.

3.4.3. Comparison with fluxes calculated from climatological averages of ice cover and wind speed. Estimates of flux from the measurements made on this expedition could be misleading if 1991 differed

Table 2. Climatological DMS fluxes for IAOE-91 reported as mean and one standard deviation ()

	Wind speed (m s ⁻¹)	K_w (cm h ⁻¹)	Fraction open water (%)	Flux ($\mu\text{mol m}^{-2} \text{day}^{-1}$)
period I	5.9 (3.5)	4.6 (5.3)	100	8.4 (10.0)
period II	5.9 (3.5)	3.9 (4.5)	17	0.45 (0.53)
period III	5.4 (3.5)	3.4 (4.3)	4	0.009 (0.015)
period IIIa	5.6 (3.5)	3.6 (4.4)	4	0.016 (0.022)
period IIIb	5.1 (3.5)	3.0 (4.2)	4	0.002 (0.003)
period IV	5.5 (3.7)	3.5 (4.5)	12	0.034 (0.046)
period V	5.5 (3.7)	4.2 (5.4)	100	0.17 (0.22)

Wind speed and fraction open water are from Vowinkel and Orvig (1970); Climate of the North Polar Basin, World Survey of Climatology, (Elsevier Science Publishing Company Amsterdam 1970). For the definition of period I-V, cf. legend, Fig. 4.

greatly from other years in the extent of ice cover and distribution of wind speeds. Fluxes were calculated as above but for climatological wind speeds and ice cover. The long term mean wind frequency distributions in Table 2 are compared with those for the individual samples of the expedition. The ships winds had a mean value (10 m in altitude) of 4.8 m s^{-1} with a standard deviation of 2.9 m s^{-1} and the climatological record had a corresponding mean and standard deviation of $5.5 \pm 3.6 \text{ m s}^{-1}$. The transfer velocities were in general lower for IAOE-91 than those indicated for historical periods. This was because wind speeds on the expedition were somewhat below the historical average. However a t-test suggests that the wind speeds were not significantly different. Ice cover for the appropriate dates was found to be greater than in 1991 but not significantly so. Therefore, the expedition fluxes could be regarded as lying within the range of year-to-year variability.

3.4.4. Estimates of potential DMS emission from the central Arctic Ocean and adjacent seas. Assuming that the observed DMS concentrations within the OWZ (summer period I; winter period V) and the CPIZ (summer period IIIa; winter period IIIb) were representative long term mean conditions we estimate the summer (May–September) and winter (October–April)

total fluxes from the major seas of the Arctic Polar Ocean (cf. Table 3). Monthly wind frequency distributions with mean and standard deviation of $5.2 \pm 3.3 \text{ m s}^{-1}$ and $4.6 \pm 3.3 \text{ m s}^{-1}$ for the summer and winter period respectively were used.

Our ($2.0 \mu\text{mol m}^{-2} \text{day}^{-1}$) summer estimate agrees well with the $2.1 \mu\text{mol m}^{-2} \text{day}^{-1}$ estimate for the region $65\text{--}80^\circ\text{N}$ by Bates et al. (1987). Their winter flux was set to zero due to the extensive ice cover, which in comparison with our estimate seems reasonable. Although the overall agreement seems excellent, large differences in the used data exist. Our calculations used on average a factor of 2 lower transfer velocity, a factor of 6 higher DMS seawater concentration and a factor of 3 higher reduction of the flux as a correction for the mean fraction of open water in the area south of 80°N .

During summer, the central Arctic Ocean contributes only 10% of the total emissions, while Greenland Sea and Kara-Barents seas make up 60% and 30%, respectively. Less than 2% of the total flux is emitted from the pack ice area. In the winter season the Greenland Sea is the major contributor (65%) of reduced sulfur to the atmosphere while about 5% was emitted from pack ice covered areas. About 30% of the total emissions came from the Kara and Barents seas. On an annual basis, winter biogenic sulfur emissions from

Table 3. DMS fluxes for the Arctic Polar Ocean (~65–90° N) reported as mean and one standard deviation ()

Region ~65–90° N	Fraction open water (%)		Area (10 ¹² m ²)		Flux (μmol m ⁻² day ⁻¹)		Emission (Gmol season ⁻¹)		Emission (Gmol year ⁻¹)	
	Summer	Winter	Summer	Winter	Summer	Winter	Summer	Winter		Total
Central Arctic Ocean	ocean	100	100	6.6	0.03	6.7 (8.7)	0.12 (0.18)	0.39	0.001	0.42
	pack ice	6	2	0.4	7.0	0.024 (0.034)	0.0013 (0.002)	0.024	0.002	
Kara and Barents sea	ocean	100	100	1.2	0.8	6.7 (8.7)	0.12 (0.18)	1.2	0.020	1.3
	pack ice	35	11	1.2	1.6	0.15 (0.21)	0.007 (0.011)	0.026	0.002	
Greenland Sea	ocean	100	100	2.1	1.9	6.7 (8.7)	0.12 (0.18)	2.2	0.049	2.2
	pack ice	21	6	0.8	1.0	0.091 (0.13)	0.004 (0.006)	0.011	0.001	
Canadian Archipelago	ocean	100	100	0.03	0	6.7 (8.7)	0.12 (0.18)	0.030	0	0.036
	pack ice	11	4	0.8	0.8	0.045 (0.064)	0.002 (0.004)	0.005	0.0004	
total	ocean	100	100	7.1	2.7	2.0* (1.7)	0.03* (0.03)	3.8	0.069	4.0
	pack ice	11	4	6.0	10.3			0.066	0.006	

Summer is defined from May to September and winter from October to April. Wind speed and fraction open water are from Vowinkel and Orvig (1970); Climate of the North Polar Basin, World Survey of Climatology (Elsevier Publishing Company Amsterdam 1970). The areas of pack ice and ocean are from Parkinson and Cavalieri (1989).

* Area weighted.

the Arctic Polar Ocean are negligible compared to the summer emissions in the region.

If concentrations of DMS similar to those found during IAOE-91 occur in the central Arctic Ocean and adjacent seas, the total flux from the Northern Hemispheric high latitudes ($\sim 65\text{--}90^\circ\text{N}$) could be about 4 Gmol yr^{-1} . Bates et al. (1992) estimated a total oceanic emission of reduced sulfur gases to the atmosphere to 480 Gmol yr^{-1} and a value of 200 for the Northern Hemisphere. From our estimates, the Arctic Polar Ocean contributes thus annually at the most 2–5% of the total flux of reduced sulfur to the Northern Hemispheric atmosphere.

In this high latitudinal regional DMS flux estimate there are several sources of uncertainty. We have defined the length of the seasons based on reported observations of phytoplankton blooms within the Arctic Polar seas, but have neglected interannual variability. Even though the calculations of K_w according to Liss and Merlivat (1986) recently has been supported by dual tracer techniques (Watson et al., 1991), other studies have suggested the Liss Merlivat relationship to underestimate K_w by about a factor 2 (Wanninkhof et al., 1993). Thus the range of potential K_w values yields $\sim 50\%$ uncertainty. Although, the DMS concentration data used in the regional extrapolation agree well with reported levels from the Greenland Sea and the Bering Sea, the seasonal relative error including the open ocean and the pack ice was $\sim 50\%$. The error in the used mean sea ice extents adds another 3% uncertainty (Parkinson and Cavalieri, 1989). Based on this analysis, the product of the uncertainties results in a factor of 2.3 uncertainty in the regional flux of DMS to the atmosphere.

4. Summary and conclusions

In order to assess both the seasonal and latitudinal variability ($75\text{--}90^\circ\text{N}$) of seawater DMS in relation to biological and hydrological parameters, and to give an estimate of the potential DMS flux to the atmosphere, we report on measurements from the open waters along the ice edge and from within the perennial pack ice of the central Arctic Ocean. The main results are as follows.

The spatial extent of high phytoplankton abundance at the IEZ and northward corresponded to the observed IEZ active melting and to

the CPIZ summer ice-melt. During the freeze-up period of the CPIZ phytoplankton biomass was low and stable probably as a consequence of extremely low availability of photosynthetic light beneath the perennial and multiple year ice.

Surface seawater DMS concentrations showed a clear seasonal progression. Highest levels were measured in the open waters in the wake of the receding ice in the beginning of August, where a potential for intense DMS production was demonstrated. Further, the importance of phytoplankton blooms and zooplankton abundance at both the IEZ and in the CPIZ during summer ice-melt to high DMS concentrations was demonstrated. Lowest DMS concentrations were measured beneath the heavy pack ice in late September.

The DMS concentrations measured during the freeze-up of the CPIZ were probably primarily due to removal processes within the water column. The turnover time of DMS in the CPIZ water column was calculated to be of the order of two weeks with the most effective sink probably of micro-biological origin.

Although, as yet limited sets of data indicated that there is a likely relationship between DMS and degraded phytoplankton material (phaeopigments), seawater DMS was not simplistically associated with phytoplankton standing stock over the large areas or different seasons covered.

The flux of DMS from the central Arctic Ocean to the atmosphere was calculated to range from close to zero up to $19 \mu\text{mol m}^{-2} \text{ day}^{-1}$ (mean $0.6 \mu\text{mol m}^{-2} \text{ day}^{-1}$), with highest fluxes confined to the open waters south of the receding ice in August. Over the pack ice area the flux of DMS was greatly reduced because of the extensive ice cover.

We have estimated the area-weighted mean summer and winter Arctic Polar Ocean flux of DMS to the atmosphere to be 2.0 and $0.03 \mu\text{mol m}^{-2} \text{ day}^{-1}$, respectively. On an annual basis, winter biogenic sulfur emissions from the mostly ice covered Arctic Polar Ocean are negligible compared to the summer emissions in the region.

The total DMS emission from the Northern Hemispheric high latitudes ($\sim 65\text{--}90^\circ\text{N}$) was estimated to be about 4 Gmol yr^{-1} , with a factor of 2.3 uncertainty. This estimate annually contributes at most 2–5% of the total flux of reduced sulfur to the Northern Hemispheric atmosphere.

Although, the major source of DMS to the

atmosphere was the open waters of the seas surrounding the mostly ice covered central Arctic Ocean, the at least 2–3 days residence time of DMS in the Arctic MBL enables it to be advected over the pack ice area. Therefore, within the pack ice, the local production of biogenic sulfur particles available for cloud formation will be primarily controlled by the extremes in environmental conditions for marine life in the open waters and along the ice edge zone of the Arctic Polar Ocean.

5. Acknowledgments

We thank the crew of the icebreaker *Oden* (chartered from the Swedish National Maritime

Administration by the Swedish Polar Research Secretariat) for their assistance and co-operation in making the expedition so successful. The authors especially thank H.-J. Hirche and his colleagues for most kindly providing the analyses of chlorophyll *a* and phaeopigments. We also thank N. Mumm, L. Anderson and G. Kattner for making the zooplankton, temperature, salinity and nutrient data available. For stimulating conversations and critical reviews of this research we wish to thank K. Bigg. We also thank P. Aalto and A. Körtzinger for technical assistance and U. Johnson for preparing the drawings. This research was founded by the Swedish Natural Science Research Council (contract E-EG/GU 9906-30/E-EG 3922-313) and The Knut and Alice Wallenberg Foundation.

REFERENCES

- Anderson, L. and Dyrssen, D. 1981. Chemical constituents of the Arctic Ocean in the Svalbard area. *Oceanol. Acta* **4**, 305–311.
- Anderson, L. G. and Jones, E. P. 1992. Tracing upper waters of the Nansen Basin in the Arctic Ocean. *Deep-Sea Res.* **39**, 425–433.
- Anderson, L. G., Björk, G., Holby, O., Jones, E. P., Kattner, G., Koltermann, K. P., Liljeblad, B., Lindgren, R., Rudels, B. and Swift, J. 1994. Water masses and circulation in the Eurasian basin. Results from the Oden 91 Expedition. *J. Geophys. Res.* **99**, 3273–3283.
- Andreae, M. O. 1986. The ocean as a source of atmospheric sulfur compounds. In: *The role of air-sea exchange in geochemical cycling* (ed. Buat-Ménard, P.). D. Reidel Dordrecht, 331–361.
- Barnard, W. R., Andreae, M. O. and Iverson, R. L. 1984. Dimethylsulfide and Phaeocystis poucheti in the south eastern Bering Sea. *Cont. Shelf. Res.* **3**, 103–113.
- Bates, T. S., Cline, J. D., Gammon, R. H. and Kelly-Hansen, S. R. 1987. Regional and Seasonal Variations in the Flux of Oceanic Dimethylsulfide to the Atmosphere. *J. Geophys. Res.* **92**, 2930–2938.
- Bates, T. S., Lamb, B. K., Guenther, A., Dignon J. and Stoiber, R. E. 1992. Sulfur Emissions to the Atmosphere from Natural Sources. *J. Atmos. Chem.* **14**, 315–337.
- Bingemer, H. 1984. *Dimethylsulfid in Ozean und mariner Atmosphäre-Experimentelle Untersuchung einer natürlichen Schwefelquelle für die Atmosphäre*. Doctoral Thesis, Berichte des Instituts für Meteorologie und Geophysik der Universität, Frankfurt am Main.
- Bolin, B. and Rodhe, H. 1973. A note on the concepts of age distribution and transit time in natural reservoirs. *Tellus* **25**, 58–62.
- Brimblecombe, P. and Shooter, D. 1986. Photo-oxidation of dimethylsulfide in aqueous solution. *Mar. Chem.* **19**, 343–353.
- Carlström, A. and Ulander, L. M. H. 1993. C-Band Backscatter Signatures of Old Sea Ice in the Central Arctic During Freeze-Up. *IEEE Transactions on Geoscience and Remote Sensing* **31**, 819–829.
- Challenger, F. and Simpson, M. I. 1948. Studies on biological methylation. Part 12: A precursor of the dimethyl-sulphide evolved by *Polysiphonia fastigata*. Dimethyl-2-carboxyethyl sulphonium hydroxid and its salt. *J. Chem. Soc.* **3**, 1591–1597.
- Challenger, F., Bywood, R., Thomas, P. and Heywood, B. J. 1957. Studies on biological methylation. XVII. The natural occurrence and chemical reactions of some thetins. *Arch. Biochem. Biophys.* **69**, 514–523.
- Charlson, R. J. and Rodhe, H. 1982. Factors controlling the acidity of natural rain water. *Nature* **295**, 683–685.
- Charlson, R. J., Lovelock, J. E., Andreae, M. O. and Warren, S. G. 1987. Oceanic phytoplankton, atmospheric sulphur, cloud albedo and climate. *Nature* **326**, 655–661.
- Cooper, W. J. and Matrai, P. A. 1989. Distribution of dimethylsulfide in the oceans. A review. In: *Biogenic sulfur in the environment* (eds. Saltzman, E. S. and Cooper, W. J.). American Chemical Society, Washington, D.C., 140–151.
- Dacey, J. W. H., Wakeham, S. G. and Howes, B. L. 1984. Henry's Law Constants for Dimethylsulfide in Freshwater and Seawater. *Geophys. Res. Lett.* **11**, 991–994.
- Dacey, J. W. H. and Wakeman, S. G. 1986. Oceanic dimethyl sulfide: production during zooplankton grazing on phytoplankton. *Science* **223**, 1314–1316.

- Deardorff, J. W. 1968. Dependence of Air-Sea transfer coefficients on bulk stability. *J. Geophys. Res.* **73**, 2549–2557.
- Dickson, D. M. J. and Kirst, G. O. 1986. The role of β -dimethylsulphoniopropionate, glycine betaine and homarine in the osmoacclimation of *Platymonas subcordiformis*. *Planta* **167**, 536–543.
- Digby, P. S. B. 1953. Plankton production in Scoresby Sound, East Greenland. *J. Animal Ecol.* **22**(2), 289–322.
- English, T. S. 1961. *Some biological oceanograph observations in the central North Polar Sea*. Sc. Rpt. 15, Res. Paper 13. Arctic Inst. North America. Calgary. 79 p.
- Fogelquist, E. 1991. Dimethylsulphide (DMS) in Wedell Sea surface and bottom water. *Mar. Chem.* **35**, 169–177.
- Gibson, J. A. E., Garrick, R. C., Burton, H. R. and McTaggart, A. R. 1990. Dimethylsulfide and the alga *Phaeocystis pouchetii* in Antarctic coastal waters. *Mar. Biol.* **104**, 339–346.
- Guest, P. S. and Davidson, K. L. 1991. The aerodynamic roughness of different types of sea ice. *J. Geophys. Res.* **96**, 4709–4721.
- Hameed, S. and Dignon, J. 1988. Changes in the geographical distributions of global emissions of NO_x and SO_x from fossil fuel combustion between 1966 and 1980. *Atmos. Environ.* **22**, 441–449.
- Hanssen, H. 1993. *Zur Verteilung des oberflächennahen Zooplanktons im europäischen Nordpolarmeer*. Masters Thesis, University of Kiel, Wischhof strasse 1–3, D-24148 Kiel, Germany, 97 p.
- Heimdal, B. R. 1983. Phytoplankton and nutrients in the waters north-west of Spitsbergen in the autumn of 1979. *J. Plankton Res.* **5**, 901–918.
- Iverson, R. L., Whiteledge, T. E. and Goering, J. J. 1979. Chlorophyll and nitrate fine structure in the southern Bering Sea shelf break front. *Nature* **281**, 664–666.
- Johannessen, O. M., Johannessen, J. A., Morison, B. A., Farrelly, B. A. and Svendsen, E. A. S. 1983. Oceanographic conditions of the marginal ice zone north of Svalbard in early fall 1979 with an emphasis on mesoscale processes. *J. Geophys. Res.* **88**, 2755–2769.
- Kanagawa, T. and Kelly, D. P. 1986. Breakdown of dimethyl sulphide by mixed cultures and by *Thiobacillus thioparus*. *FEMS Microbiol. Lett.* **34**, 13–19.
- Kattner, G. and Becker, H. 1991. Nutrients and organic nitrogenous components in the marginal ice zone of the Fram Strait. *J. Mar. Syst.* **2**, 385–394.
- Keller, M. D., Bellows, W. K. and Guillard, R. R. L. 1989. Dimethyl sulfide production in marine phytoplankton. In: *Biogenic sulfur in the environment* (eds. Saltzman, E. S. and Cooper, W. J.). American Chemical Society, Washington, D.C., 183–200.
- Kiene, R. P. and Bates, T. S. 1990. Biological removal of dimethyl sulfide from sea water. *Nature* **345**, 702–704.
- Kiene, R. P. 1992. Dynamics of dimethyl sulfide and dimethylsulfonic propionate in oceanic water samples. *Mar. Chem.* **37**, 29–52.
- Kirst, G. O., Thiel, C., Wolff, H., Nothnagel, J., Wanzek, M. and Ulmke, R. 1991. Dimethylsulphoniopropionate (DMSP) in ice-algae and its possible biological role. *Mar. Chem.* **35**, 381–388.
- Leck, C. and Bågander, L.-E. 1988. Determination of Reduced Sulfur Compounds in Aqueous Solutions Using GC/FPD. *Anal. Chem.* **60**, 1680–1683.
- Leck, C., Larsson, U., Bågander, L.-E., Johansson, S. and Hajdu, S. 1990. DMS in the Baltic Sea—Annual variability in relation to biological activity. *J. Geophys. Res.* **95**, 3353–3363.
- Leck, C. and Rodhe, H. 1991. Emissions of marine biogenic sulfur to the atmosphere of Northern Europe. *J. Atmos. Chem.* **12**, 63–86.
- Leck, C. and Persson, C. 1996. Seasonal and short-term variability in dimethyl sulfide, sulfur dioxide and biogenic sulfur and sea salt aerosol particles in the arctic marine boundary layer during summer and autumn. *Tellus* **48B**, this issue.
- Liljeström, G. 1992. *Ice-breaker Oden trafficability data report: International Arctic Ocean Expedition 1991*. Swedish Arctic Research Programme, Swedish Polar Research Secretariat, Box 50005, S-10405 Stockholm, Sweden.
- Liss, P. S. and Slater, P. G. 1974. Flux of gases across the air-sea interface. *Nature* **247**, 181–184.
- Liss, P. S. and Merlivat, L. 1986. Air-sea gas exchange rates: introduction and synthesis. In: *The role of air-sea exchange in geochemical cycling* (ed. Buat-Ménard, P.). Reidel, Dordrecht, 113–127.
- Maykut, G. A. and Grenfell, T. C. 1975. The spectral distribution of light beneath first-year sea ice in the Arctic Ocean. *Limnol. Oceanogr.* **20**, 554–563.
- Möller, D. 1984. Estimation of the global man-made sulphur emission. *Atmos. Environ.* **18**, 19–27.
- Nguyen, B. C., Belviso, S., Mihalopoulos, N., Gostan, J. and Nival, P. 1988. Dimethyl sulfide production during natural phytoplankton blooms. *Mar. Chem.* **24**, 133–141.
- Niebauer, H. J. and Alexander, V. 1985. Oceanographic frontal structure and biological production at an ice-edge. *Cont. Shelf Res.* **4**, 367–388.
- Nilsson, E. D., 1996. Planetary boundary layer structure and air mass transport during the International Arctic Ocean Expedition, 1991. *Tellus* **48B**, this issue.
- Parkinson, C. L. and Cavalieri, D. J. 1989. Arctic Sea Ice 1973–1987: Seasonal, Regional, and Interannual Variability. *J. Geophys. Res.* **94**, 14499–14523.
- Sakshaug, E. and Slagstad, D. 1991. Light and productivity of phytoplankton in polar marine ecosystems: a physiological view. *Polar Res.* **10**, 69–85.
- Saltzman, E. S., King, D. B., Holmén, K. and Leck, C. 1993. Experimental Determination of the Diffusion Coefficient of Dimethyl Sulfide in Water. *J. Geophys. Res.* **98**, 16,481–16,486.
- Smith, W. O. and Nelson, D. M. 1985. Phytoplankton Bloom produced by a Receding Ice Edge in the Ross Sea: Spatial Coherence with the Density Field. *Science* **227**, 163–166.

- Spiro, P. A., Jacob, D. J. and Logan, J. A. 1992. Global inventory of sulfur emissions with $1^{\circ} \times 1^{\circ}$ resolution. *J. Geophys. Res.* **97**, 6023–6036.
- Staubes, R. and Georgii, H.-W. 1993. Measurements of atmospheric and seawater DMS concentrations in the Atlantic, the Arctic and Antarctic region. In: *Commission of the European Communities: Dimethylsulphide: Oceans, atmosphere and climate*. Proceedings of International Symposium held in Belgrate, Italy, 13–15 October 1992 (eds. G. Restelli and G. Angelletti), Kluwer Academic Publishers, 95–102.
- Svedrup, H. U. 1953. On conditions for the vernal blooming of phytoplankton. *J. Cons. Perm. Int. Explor. Mer.* **18**, 287–295.
- Turner, S. M., Malin, G., Liss, P. S., Harbour, D. S. and Holligan, P. M. 1988. The seasonal variation of dimethyl sulfide and dimethylsulfoniopropionate concentrations in near-shore waters. *Limnol. Oceanogr.* **33**, 364–375.
- Vairavamurthy, A., Andreae, M. O. and Iverson, R. L. 1985. Biosynthesis of dimethylsulfide and dimethylpropiothetin by *Hymenomonas carterae* in relation to sulfur source and salinity variations. *Limnol. Oceanogr.* **30**, 59–70.
- Vowinckel, E. and Orvig, S. 1970. *Climate of the north polar basin, world survey of climatology*. Elsevier Science Publishing Company, Amsterdam, 1970.
- Wanninkhof, R. 1992. Relationship between wind speed and gas exchange over the ocean. *J. Geophys. Res.* **97**, 7373–7381.
- Wanninkhof, R., Asher, W., Weppernig, R., Chen, H., Schlosser, P., Langdon, C. and Sambrotto, R. 1993. Gas transfer experiment on Georges Bank using two volatile deliberate tracers. *J. Geophys. Res.* **98**, 20,237–20,248.
- Watson, J. A., Upstill-Goddard, R. C. and Liss, P. S. 1991. Air-sea gas exchange in rough and stormy seas measured by a dual-tracer technique. *Nature* **349**, 145–147.